Available online at www.sciencedirect.com

ScienceDirect

Procedia Computer Science 100 (2016) 1305 – 1312

Procedia Computer Science

Conference on ENTERprise Information Systems / International Conference on Project MANagement / Conference on Health and Social Care Information Systems and Technologies, CENTERIS / ProjMAN / HCist 2016, October 5-7, 2016

Sentinel-1 Support in the GAMMA Software

Urs Wegnüller, Charles Werner, Tazio Strozzi, Andreas Wiesmann, Othmar Frey, and Maurizio Santoro*

Gamma Remote Sensing AG, Worbstrasse 225, 3073 Gümligen, Switzerland

Abstract

First results using the new Sentinel-1 SAR look very promising but the special interferometric wide-swath data acquired in the TOPS mode makes InSAR processing more challenging than for normal stripmap mode data. The steep azimuth spectra ramp in each burst results in very stringent co-registration requirements. Combining the data of the individual bursts and sub-swaths into consistent mosaics requires careful "book-keeping" in the handling of the data and meta data and the large file sizes and high data throughputs require also a good performance. Considering these challenges good support from software is getting increasingly important. In this contribution we describe the Sentinel-1 support in the GAMMA Software, a high-level software package used by researchers, service providers and operational users in their SAR, InSAR, PSI and offset tracking work.

© 2016 The Authors. Published by Elsevier B.V. This is an open access article under the CC BY-NC-ND license (http://creativecommons.org/licenses/by-nc-nd/4.0/).
Peer-review under responsibility of the organizing committee of CENTERIS 2016
Keywords: Sentinel-1; InSAR; PSI; offset tracking;split-beam interferometry; GAMMA Software

1. Introduction

On 3. April 2014 ESA launched the first of the two Sentinel-1 (S1) satellites with the interferometric wide-swath (IWS) mode selected as the main acquisition mode. In IWS mode, the data are acquired using the so-called TOPS mode [1]. TOPS stands for Terrain Observation with Progressive Scans in azimuth. One of the strengths of the IWS mode is the wide swath width of about 250km. S1 is operated at C-band with an orbit repeat cycle of 12 days. In combination with S1B, successfully launched in spring 2016, this reduces to 6 days.

* Corresponding author. Tel.: +41-31-9517005; fax: +41-31-9517008.
E-mail address: wegmuller@gamma-rs.ch.

1877-0509 © 2016 The Authors. Published by Elsevier B.V. This is an open access article under the CC BY-NC-ND license (http://creativecommons.org/licenses/by-nc-nd/4.0/).
Peer-review under responsibility of the organizing committee of CENTERIS 2016
doi:10.1016/j.procs.2016.09.246

The orbital tube is very narrow (of the order of 100m) and the TOPS mode bursts are almost perfectly synchronized to support SAR Interferometry (InSAR).

The GAMMA Software is a high-level software package that supports researchers, service providers and operational users in their SAR, InSAR, and PSI (Persistent Scatterer Interferometry) related work. In this contribution, we describe the support the GAMMA Software provides for interferometry, offset tracking and PSI using S1 IWS data and the related procedures used.

2. S1 IWS data handling and basic functionality

S1 IWS data are available as RAW, SLC (Single Look Complex) and GRD (Ground Range Dataset) products. S1 IWS RAW data are distributed for specific usage only. Currently, the use of S1 IWS SLC and GRD data is supported in the GAMMA Software. The GRD products can be imported, calibrated and geocoded in the GAMMA Software. The GRD products may be used to analyze the backscattering coefficient and for offset tracking, e.g. to map glacier motion.

The S1 IWS SLC product is a set of three "burst SLC", each one including a number of bursts over one of the sub-swaths. An example of a burst SLC of sub-swath IW1 is shown in Figure 1. The area covered by the individual bursts overlaps in both azimuth (between sub-sequent bursts) and range (between neighboring sub-swaths), as sketched in Figure 2. In the GAMMA Software the S1 IWS SLC product is imported and stored as "burst SLC" consisting of the image data of the 3 sub-swaths and related parameter files containing the relevant metadata. In the importing step, the radiometric calibration is applied. Functionality to process the "burst SLC" includes the possibility to generate a mosaic SLC and a mosaic MLI (Multi-Look Intensity image, Figure 3). In both cases, this is a single data file with a single parameter file. The data are cut in the overlap region such that only pixels (looks) from the same burst and sub-swath are combined into a MLI pixel. Geometrically and radiometrically the S1 IWS SLC have a very high standard, so that the generated mosaics are typically seamless in both range and azimuth. MLI mosaics can be geocoded using the normal procedure used in the GAMMA Software. The S1 state vectors distributed with the data can be used or OPOD precision state vectors that become available some days after the acquisition can be added. Typically, co-registration accuracies of a few meter or better are achieved, even without applying a refinement to the geocoding. In addition, the GAMMA Software includes programs to extract the SLC data of a single burst into an individual SLC mosaic data file with a corresponding parameter file and to remove the azimuth spectrum variation related phase ramp from burst SLCs or individual bursts.

3. S1 IWS Interferometry

For TOPS interferometry an extremely accurate co-registration accuracy in the azimuth direction of a few thousandths of a pixel is absolutely required [2], otherwise phase jumps between subsequent bursts are observed. To assure this required co-registration accuracy we use a method that considers the effects of the scene topography. Furthermore, a refinement of the transformation is determined, typically, including first a matching procedure and then a spectral diversity method [3] that considers the interferometric phase of the burst overlap region. The refinement applied for a larger image section including all 3 sub-swaths and multiple bursts is a constant offset in slant range and in azimuth.

A differential interferogram calculated after the refinement with the matching procedure (accuracy of the order of 1/100 azimuth pixel) is shown in Figure 4 and the final differential interferogram after refinement with the spectral diversity method is shown in Figure 5. In the following, phase filtering, phase unwrapping, e.g. using a minimum cost-flow approach, phase to displacement conversion and coherence estimation are the same as for conventional stripmap interferometry. The corresponding geocoded RGB composite of the coherence (red), the backscatter (green) and the backscatter change (blue) is shown in Figure 6.

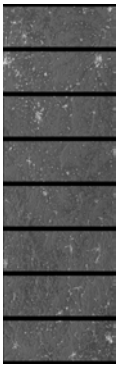


Fig. 1 IW1 SLC bursts

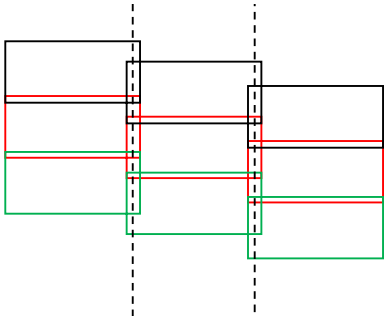


Fig. 2 S1 burst structure with small overlaps between bursts and sub-swaths.

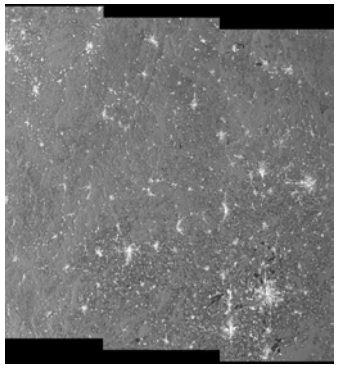


Fig. 3 MLI mosaic for a “full Sentinel-1 TOPS scene” consisting of 3 sub-swaths with 10 bursts each.

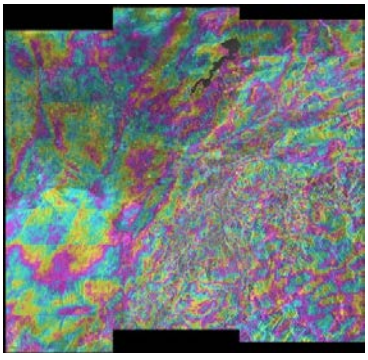


Fig. 4 S1 TOPS differential interferogram after the matching co-registration refinement. Phase jumps are clearly visible between some consecutive bursts.

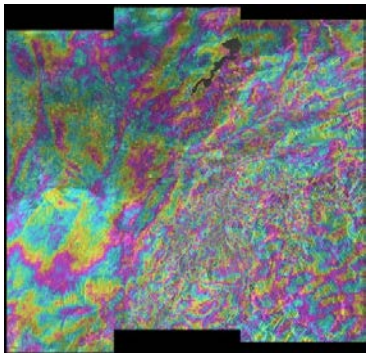


Fig. 5 S1 TOPS differential interferogram as obtained after the spectral diversity co-registration refinement. The phase matches well between bursts and adjacent sub-swaths.

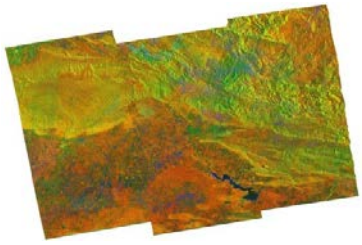
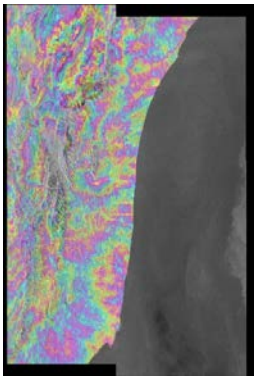
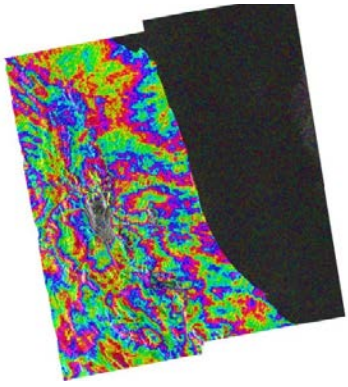


Fig. 6 S1 IWS geo-referenced RGB composite of the coherence (red), the backscatter (green) and the backscatter change (blue).





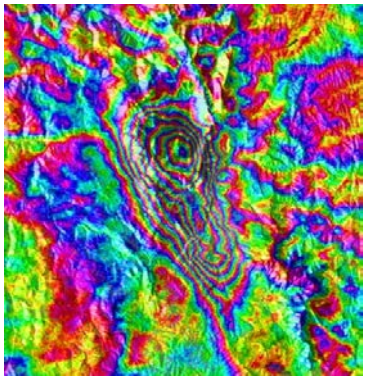


Fig. 7 Co-seismic 6-day S1A – S1B TOPS differential interferogram (ascending orbits, 20160822 – 20160828) over central Italy. The image to the left shows the complex valued differential interferogram, the image in the center the unwrapped and slightly filtered differential interferometric phase (using a cyclic color scale with 6.28 radian per color cycle, i.e. corresponding to the wrapped phase), and the image to the right shows an enlarged section with the main deformation pattern.

The exact same procedure also works for cross-sensor interferograms between Sentinel-1A (S1A) and Sentinel-1B (S1B) which was launched on 25-Apr-2016. A significant advantage of having both satellites available is that interferograms for a shorter 6-day temporal baseline can be formed. An example of an S1A – S1B differential interferogram is shown in Figure 7 for the co-seismic displacement of the Earthquake that took place in central Italy on 24-Aug-2016.

4. Interferometric time series analysis

In the GAMMA IPTA Software a broad range of tools supporting different interferometric time series analysis approaches are supported, using either single or multi-looked interferometric phase and using either single reference or multi reference stacks to derive the deformation time series. For initial tests with S1 IWS data we used a stack over Mexico City, consisting of a relatively small number of 12 repeat observations. Because of the small stack and the very significant ground motion in the Mexico City area we used multi-reference stacks for both the SBAS (Small Baseline Differential SAR Interferometry) and PSI processing done.

As input to the time series analysis we co-registered all the S1 IWS SLC to one selected reference scene (20151015). This was done using the procedure described in section 3, including the refinement with the spectral diversity method. This worked well as confirmed by differential interferogram mosaics without visible phase jumps at burst interfaces and between sub-swaths and with generally very high coherence over urban areas. For the SBAS and PSI processing we deramped the co-registered SLC mosaics for the azimuth phase ramps and cut out a common 16000 x 5000 pixel section over Mexico city. In the following the SBAS and PSI procedures used and the results achieved are discussed.

4.1. SBAS time series analysis with S1 IWS data

We followed an SBAS procedure similar to the one described in [7,8]. In particular we considered multi-looked differential interferometric phases using 10 range and 2 azimuth looks. For the entire stack all the baselines are below 250m and so all spatial baselines are short. To maximize the temporal coherence but also to facilitate the phase unwrapping by minimizing the deformation phase we considered the shortest time intervals possible. As we wanted to include redundant observations we decided to include all pairs between scenes that are up to 3 positions away from each other in the time series (i.e. 1-2, 1-3, 1-4, 2-3, 2-4, 2-5, 3-4, …), which resulted in a total of 30 pairs.

For each pair we calculated the differential interferogram using the Shuttle Radar Topographic Mission (SRTM) height as topographic reference and unwrapped the phase. The unwrapped phases were then converted to a time-series using singular value decomposition. Besides the phase time series quality information such as the phase standard deviation from the time series is provided. For areas where an unwrapping error occurred phase standard deviation from the time series get significantly higher and so the result in these areas can be excluded from the solution. The main results are the average deformation rate (Figures 8) and the deformation time series. Converting the line-of-sight values to a vertical displacement rate (assuming the movement is in the vertical direction) we observed maximum subsidence rates of more than 40cm/year. No anomalies were observed at the interface between subsequent bursts. Besides, height corrections were estimated in the Singular Value Decomposition (SVD) step.

4.2. PSI time series analysis with S1 IWS data

The co-registered deramped SLC mosaic stack over Mexico City can be used as input to a PSI processing in the same way as used for conventional stripmap mode data. In the identification of persistent scatterer candidates, we applied a spectral diversity criteria as well as criteria on the backscatter variability and level [4].

The spectral diversity method available in the GAMMA IPTA software for the identification of point-like scatterers can be used as well as range oversampling of the SLCs if the SLCs are deramped.

Thanks to the good range resolution of the S1 IWS data a high number of suited persistent scatterers was identified. In urban areas the point density was often significantly larger than 1000 points/km^2. To make the PSI processing more efficient, especially if processing large areas, we initially reduce the candidate list size using the methodology described in [5]. This is done adaptively, such that the point density is strongly reduced in areas with a very high point density while not reduced at all in areas with a low point density. The fact that only the vector data stacks are used in most IPTA programs means that the relevant parameter for the speed of a processing step is not the size of the area or of the full SLC but only the number of points in the point candidate list. This makes the IPTA approach very efficient for S1 IWS PSI. Because of the limited number of scenes included we used the same multi-reference stack as used in the SBAS processing. Using this multi-reference stack we estimated point height corrections, linear deformation rates and atmospheric phases. These initial linear deformation rate estimates are not of very high quality because they are based on the short interval pairs. Besides of these parameters this step also provides the unwrapped phase components. These component are then added to get the total point differential phases for the multi-reference stack. SVD is then used to convert the multi-reference stack phases to a single reference time series. Further processing may be done on this result considering the single reference stack. In this example this was not done because of the small stack size. In other examples single reference stack PSI approaches were also successfully used.

The average deformation rate derived in the PSI processing (Figure 9) corresponds closely to the result of the SBAS processing (Figure 8). Considering stable areas shows that mm/year precision is clearly not reached with this C-band stack of 12 scenes between October 2014 and March 2015. In this PSI result no anomalies were observed at the interface between subsequent bursts.

In the above described PSI method only data of one burst is considered in the burst overlap (and sub-swath overlap) regions. This seems reasonable as it results in spatially consistent point densities. Nevertheless, to specifically investigate how points behave in the two different bursts (or sub-swaths) of an overlap area the programs to extract SLCs of single bursts can be used.

5. S1 IWS offset tracking

To apply offset tracking for S1 TOPS mode SLC data the basic strategy is to first co-register the two burst SLC as described in Section 3. In order to apply oversampling in the offset tracking procedures it is recommended to first deramp the SLC data for the azimuth phase ramp. Further processing (quality control, geocoding, conversion to displacements in meters, visualization) is then done as for normal stripmap mode data. An example of a glacier velocity map over a part of Greenland is shown in Figure 10. As compared to ENVISAT ASAR the sensitivity is improved in range direction thanks to the higher S1 range. On the other hand the resolution is lower in azimuth direction as a consequence of the lower azimuth resolution of the IWS data.

For S1 TOPS mode GRD data offset tracking can be applied using the procedure as for strip-map mode data. The main interest in offset tracking is to map displacements. But azimuth offsets may also be of interest to identify ionospheric effects [6, see also Section 6 and Figure 12] or for radargrammetry.

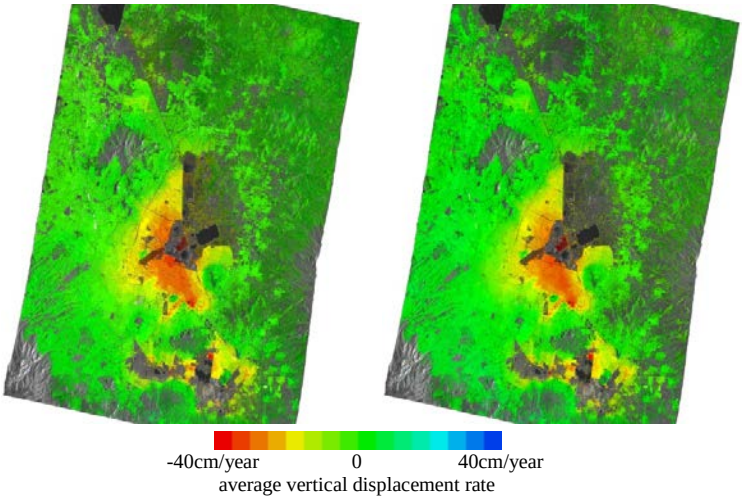


Fig. 8 Average vertical displacement rate derived from a stack of 12 S1 IWS SLC over Mexico City using an SBAS procedure

Fig. 9 Average vertical displacement rate derived from a stack of 12 S1 IWS SLC over Mexico City using a PSI procedure.

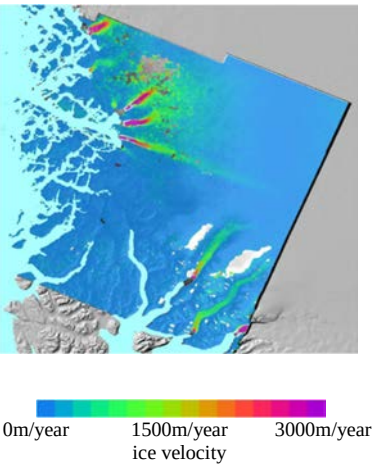


Fig. 10 Velocity map of the Upernvaik area overlaid the shaded relief of the Greenland Mapping Project (GIMP) DEM [10].

6. Split-beam interferometry (SBI)

In the S1 SLC co-registration procedure described above the SBI in the burst overlap between the different bursts is used to determine the final co-registration refinement in the azimuth direction. SBI within bursts is also of interest to identify ionospheric effects [6]. For this the co-registered burst SLCs are deramped for the Doppler ramp. Then the normal SBI methodology that includes band-pass filtering to generate sub-band SLCs, 1-look interferogram generation for sub-band interferograms, and calculation and multi-looking of double difference interferogram. A split-beam interferogram example over Devon Ice Cap, Canada, clearly affected by ionospheric effects, is shown in Fig. 11, together with the corresponding azimuth offset map in Fig. 12 that confirms the ionospheric origin of the phase streaks.

7. Conclusions

The procedures used in the GAMMA Software for interferometry, offset tracking and interferometric time series analysis (SBAS and PSI) using S1 IWS data were described. The main differences to “normal” strip map mode data are the organization of the IWS SLC data in 3 sub-swaths and by burst, and the extremely accurate co-registration accuracy required for interferometry to avoid phase jumps between consecutive bursts (caused by the strong along-track Doppler Centroid variation). As a consequence much more care is taken with the co-registration procedure also including new elements as the use of a spectral diversity method applied to the burst overlap areas. The results achieved confirm that the S1 IWS data are well suited for interferometry, offset tracking and interferometric time series analysis. Besides the presented SBAS and PSI approach other time series approaches, e.g. working with a single reference stack or methods combining single and multi-look interferometric phases [9] are also applicable, especially with larger stacks becoming available.

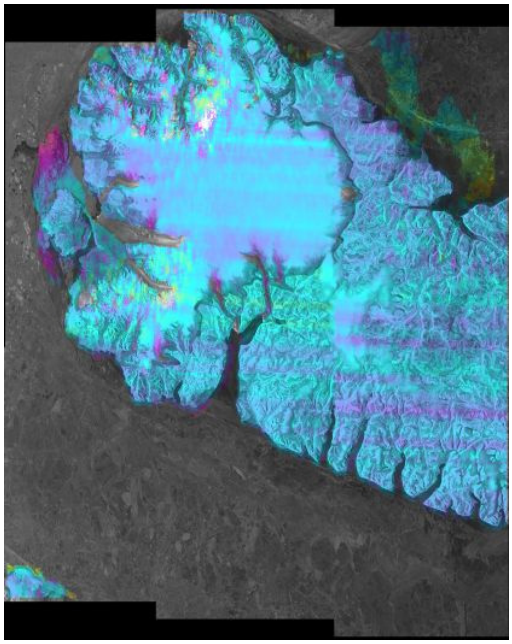


Fig. 11 Devon Ice Cap, Canada. Azimuth offsets between S1 IWS data of 20150117 and 20150129 showing "ionospheric azimuth streaking" of the order of 0.1 SLC pixel.

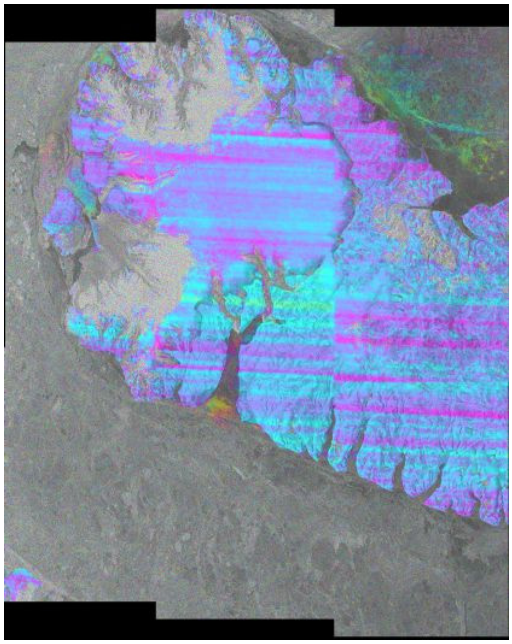


Figure 12 Devon Ice Cap, Canada. Split beam interferometric phase of S1 IWS pair of 20150117 and 20150129 showing "ionospheric azimuth streaking" of the order of 0.5 radian.

Acknowlegments

This work contains modified Copernicus data (Sentinel-1).

References

[1] De Zan F. and A. Guarnieri, Terrain Observation by Progressive Scans, IEEE TGRS, vol. 44, no. 9, pp. 2353-2360, 2006.
[2] Prats P., L. Marotti and R. Scheiber, Investigation on TOPS Interferometry with TerraSAR-X, Proc. of IGARSS 2010.
[3] Scheiber R. and A. Moreira, Coregistration of interferometric SAR images using spectral diversity, TGRS, vol. 38, no. 5, pp. 2179–2191, 2000.
[4] Werner C., U. Wegmüller, T. Strozzi, and A. Wiesmann, "Interferometric point target analysis for deformation mapping", Proc. IGARSS 2003, Toulouse, France, 21-25 July 2003.
[5] Wegmüller U., O. Frey, and C. Werner, "Point Density Reduction in Persistent Scatterer Interferometry", Procs. EUSAR 2012 Conf., 24-26. Apr. 2012.
[6] Wegmüller U., T. Strozzi, and C. Werner, Ionospheric path delay estimation using split-beam interferometry, Procs. IGARSS'2012, Munich, Germany, 22-27 July 2012.
[7] Berardino, P., Fornaro, G., Lanari, R., Member, S., & Sansosti, E., A New Algorithm for Surface Deformation Monitoring Based on Small Baseline Differential SAR Interferograms. IEEE TGRS, 40(11), 2375–2383, 2002.
[8] Lanari, R., Member, S., Mora, O., Manunta, M., Mallorquí, J. J., Berardino, P., & Sansosti, E., A Small-Baseline Approach for Investigating Deformations on Full-Resolution Differential SAR Interferograms. IEEE TGRS, 42(7), 1377–1386. 2004.
[9] Kourkouli, P., Wegmüller, U., Teatini, P., Tosi, L., Strozzi, T., Wiesmann, A., & Tansey, K., Ground Deformation Monitoring Over Venice Lagoon Using Combined DInSAR/PSI Techniques. In G. Lollino, A. Manconi, J. Locat, Y. Huang, & M. Canals Artigas

(Eds.), Eng. Geology for Society and Territory – Vol. 4 SE - 35 (pp. 183–186). Springer International Publishing. doi:10.1007/978-3-319-08660-6_35, 2014.

[10] Howat, I.M., A. Negrete, B.E. Smith, 2014, The Greenland Ice Mapping Project (GIMP) land classification and surface elevation datasets, The Cryosphere, 8, 1509-1518, doi:10.5194/tc-8-1509-2014.